



OPEN

Age-related long-term response in rat thyroid tissue and plasma after internal low dose exposure to ^{131}I

Malin Larsson^{1✉}, Nils-Petter Rudqvist^{1,2,3}, Johan Spetz^{1,4}, Toshima Z. Parris⁵, Britta Langen^{1,6}, Khalil Helou⁵ & Eva Forssell-Aronsson^{1,7}

^{131}I is used clinically for therapy, and may be released during nuclear accidents. After the Chernobyl accident papillary thyroid carcinoma incidence increased in children, but not adults. The aims of this study were to compare ^{131}I irradiation-dependent differences in RNA and protein expression in the thyroid and plasma of young and adult rats, and identify potential age-dependent biomarkers for ^{131}I exposure. Twelve young (5 weeks) and twelve adult Sprague Dawley rats (17 weeks) were i.v. injected with 50 kBq ^{131}I (absorbed dose to thyroid = 0.1 Gy), and sixteen unexposed age-matched rats were used as controls. The rats were killed 3–9 months after administration. Microarray analysis was performed using RNA from thyroid samples, while LC–MS/MS analysis was performed on proteins extracted from thyroid tissue and plasma. Canonical pathways, biological functions and upstream regulators were analysed for the identified transcripts and proteins. Distinct age-dependent differences in gene and protein expression were observed. Novel biomarkers for thyroid ^{131}I exposure were identified: (PTH), age-dependent dose response (CA1, FTL1, PVALB (youngsters) and HSPB6 (adults)), thyroid function (*Vegfb* (adults)). Further validation using clinical samples are needed to explore the role of the identified biomarkers.

Thyroid diseases are routinely examined or treated with ^{131}I , due to natural physiological uptake of iodine. However, ionizing radiation can also induce cancer in normal cells. During the Chernobyl accident, large amounts of radioactive nuclides were released into the atmosphere, including over 1.8 EBq of ^{131}I activity¹. The absorbed dose to thyroid from ^{131}I was then higher in children in the most contaminated areas (ca 900 mGy and 170 mGy for evacuated and non-evacuated children and adolescents) than adults, which may partly explain why more papillary thyroid cancer (PTC) cases (> 5000 during 1992–2005) were detected in children but not adults². Children are also likely more sensitive to radiation than adults, due to higher more active cellular proliferation, with cells more often in sensitive cell cycle phases (M and G2 phase)^{3,4}. Epidemiological studies on thyroid cancer risks have been performed and reviewed^{5,6}. Furthermore, children and young adults that received ^{131}I for diagnostic purposes had a higher risk of developing secondary malignancies, besides having longer expected lifespans⁷. However, a large Swedish study demonstrated no excess risk for thyroid cancer in adults after diagnostic exposure to ^{131}I ⁸. Nevertheless, our understanding of the long-term effects of ^{131}I exposure in thyroid tissue is limited and more knowledge is needed.

In recent years, efforts were made to identify tissue-specific molecular markers (biomarkers), e.g. proteins and RNA transcripts that can predict previous radiation exposure, altered thyroid function, and cancer induction. Traditionally, immunohistopathology was the method of choice⁹. Lately, several alternative methods were

¹Department of Medical Radiation Sciences, Institute of Clinical Sciences, Sahlgrenska Center for Cancer Research, Sahlgrenska Academy, University of Gothenburg, 413 45 Gothenburg, Sweden. ²Department of Thoracic/Head and Neck Medical Oncology, University of Texas MD Anderson, Houston, TX 77030, USA. ³Department of Immunology, University of Texas MD Anderson, Houston, TX 77030, USA. ⁴John B. Little Center for Radiation Sciences, Harvard T. H. Chan School of Public Health, Boston, MA 02115, USA. ⁵Department of Oncology, Institute of Clinical Sciences, Sahlgrenska Center for Cancer Research, Sahlgrenska Academy, University of Gothenburg, 413 45 Gothenburg, Sweden. ⁶UT Department of Radiation Oncology, Division of Molecular Radiation Biology, UT Southwestern Medical Center, 2201 Inwood Rd., Dallas, TX 75390, USA. ⁷Department of Medical Physics and Biomedical Engineering, Sahlgrenska University Hospital, 413 45 Gothenburg, Sweden. ✉email: malin.larsson@gu.se

introduced, e.g. genetic profiles, including single nucleotide polymorphisms (SNPs), and gene and protein expression^{10–14}. To study the impact of irradiation on thyroid tissue, tumour material from patients irradiated after the Chernobyl accident were analysed. Genotyping of PTC tissue showed that SNPs in *ATM* exon 39 and *XRCC1* exon 10 were potential biomarkers of decreased PTC risk in adults, and *ATM* IVS22-77 and *TP53* codon 72 were associated with radiation exposure¹⁵. Based on PTC tissue from children, the CLIP2 protein was proposed as a radiation-induced biomarker^{12,16}. The thyroglobulin (TG) protein level in blood was previously proposed as a biomarker for externally irradiated thyroid during childhood^{17,18}. TG blood levels may also be related to thyroid size and function rather than type of thyroid malignancy, and its potential as a cancer biomarker needs to be further evaluated¹⁹.

We have previously proposed the *Agpat9*, *Klk1*, *Klk1b* family, *Plau*, *Prf1*, and *S100a8* genes as biomarkers for ¹³¹I exposure in adult mouse thyroid tissue using transcriptomic and proteomic analyses^{20–23}. We also showed that circadian rhythm affected gene expression patterns in the thyroid, with a strong association with the kallikrein gene family²¹. Recently, we investigated the biological effects on thyroid tissue nine months after ¹³¹I injection in young rats (thyroid absorbed dose of 0.01–1 Gy)²⁴. Several significant ¹³¹I exposure-related RNA transcripts (*Afp* and *RT1-Bb*) and proteins (ARF3, DLD, IKBKB, NONO, RAB6A, RPN2, and SLC25A5), and absorbed dose-related biomarkers (APRT, DSG4, LDHA, and TGM3) were identified. Candidate biomarkers for changes in thyroid function were also proposed: ACADL, SORBS, TPO and TG proteins. These data demonstrate the importance of directly comparing age-related long-term differences in radiobiological response to ¹³¹I exposure.

The aims of this work were to (a) identify differences in expression patterns on the RNA and protein levels in young and adult rats exposed to ¹³¹I, and (b) identify potential biomarkers related to ¹³¹I exposure and thyroid function.

Results

The six groups of Sprague Dawley rats exposed to ¹³¹I are hereafter denoted as 3 months young (Y3), 6 months young (Y6), 9 months young (Y9), 3 months adult (A3), 6 months adult (A6), and 9 months adult (A9) rats. When combining data from two or three groups, abbreviations were used, such as Y3 + Y6 as a shortening for the Y3 and Y6 groups together.

Time-related RNA expression profiles in irradiated versus non-irradiated young rats. RNA microarray analysis identified 252 differentially regulated transcripts (corresponding to 243 genes) in the irradiated thyroids of young rats (Fig. 1a), of which 91, 43, and 25 transcripts (90, 43, and 24 genes) were unique for the Y3, Y6, and Y9 groups, respectively (Supplementary Table S1). Twenty RNA transcripts with the highest differential regulation are presented in Fig. 2a. The *Tpo* (Y3), *Klhl14* and *Tg* (Y6) genes encode for the TPO, KLHL14 and TG proteins that are involved in thyroid function according to the Human Protein Atlas (HPA) (Supplementary Table S2). No RNA transcript was differentially regulated in all three groups for young individuals. However, 93 RNA transcripts (86 genes) were commonly regulated in the Y3 and Y6 groups (Fig. 1a).

Mass spectrometry analysis identified 631 proteins associated with ¹³¹I exposure in young rat thyroid tissue (Fig. 1b), of which 83, 233, and 158 unique proteins were identified in the Y3, Y6, and Y9 groups, respectively (Supplementary Table S3). Only the OCLN (Y6) and SORBS2 (Y9) proteins were highly associated with thyroid function according to HPA (Supplementary Table S2). Twenty proteins with the highest differential expression levels are presented in Fig. 2b. In total, 141 proteins were identified in at least two groups, of which ACADL was thyroid-related (Y6 + Y9) (Supplementary Table S2). Altogether 36 and 10 proteins were found for the Y3 + Y6 and Y6 + Y9 groups, respectively, and showed uniformly increased or decreased expression levels (Fig. 2). Sixteen proteins with altered expression patterns at all three time points were identified (APMAP, CPT2, DECR1, FABP4, FABP5, GDI2, HMMR, KRT4, KRT13, KRT15, LGALS7, MLEC, PTH, RAP1A, TKT, and TUFM; Fig. 3).

In plasma from irradiated young rats, 328 proteins were identified, of which 50, 123, and 66 proteins were unique in the Y3, Y6, and Y9 groups, respectively (Fig. 1c, Supplementary Table S4). Twenty proteins with highest differential expression levels are presented in Fig. 2. None of these proteins was associated with thyroid function according to HPA. In total, 77 proteins were present in two of the three groups, and the proteins with uniformly increased or decreased expression levels for Y3 + Y6 and Y6 + Y9 groups are presented in Fig. 2. Twelve differentially expressed proteins were detected in all groups (CA1, CAPN1, eEF1A1, F7, FTL1, GPD1, PF4, PLEC, PKLR, PROC, PVALB, and RGS18; Fig. 3). The CA1 protein had uniformly increased expression level, and the FTL1 and PVALB proteins revealed uniformly decreased expression levels for all three groups.

Time-related expression profiles in irradiated versus non-irradiated adult rats. In total, 456 differentially regulated transcripts (corresponding to 426 genes) were identified in the irradiated thyroid tissue of adult rats using RNA microarray analysis, with 16, 18 and 412 RNA transcripts (16, 18 and 382 genes) uniquely detected in the A3, A6, and A9 groups, respectively (Fig. 1d, Supplementary Table S5). Twenty RNA transcripts with the highest regulation are presented in Fig. 2. According to HPA, the *Tg* (A3) and *Marvel2*, *Sorcs1*, *Ipcpe1* and *Irs4* (A9) genes were thyroid-related (Supplementary Table S2). Only the *Vegfb* transcript was significantly regulated in all adult groups (A3, A6, and A9). However, *Vegfb* was up-regulated in the A3 and A6 groups and down-regulated in the A9 group (Fig. 3). The *Vegfb* and *Klk1c9* transcripts were uniformly expressed in the A3 + A6 group (Fig. 2).

A total of 806 differentially expressed proteins were detected in adult thyroid tissue using LQ-MS/MS analysis, with 444, 142 and 43 unique proteins identified in the A3, A6 and A9 groups, respectively (Fig. 1e, Supplementary Table S6). The 20 proteins with highest expression levels are presented in Fig. 2. The OCLN (A3) was the only protein associated with thyroid function according to HPA (Supplementary Table S2). Only two of the 165 proteins detected in two groups were thyroid-specific, i.e. ACADL (A3 + A6) and TG (A6 + A9) (Supplementary

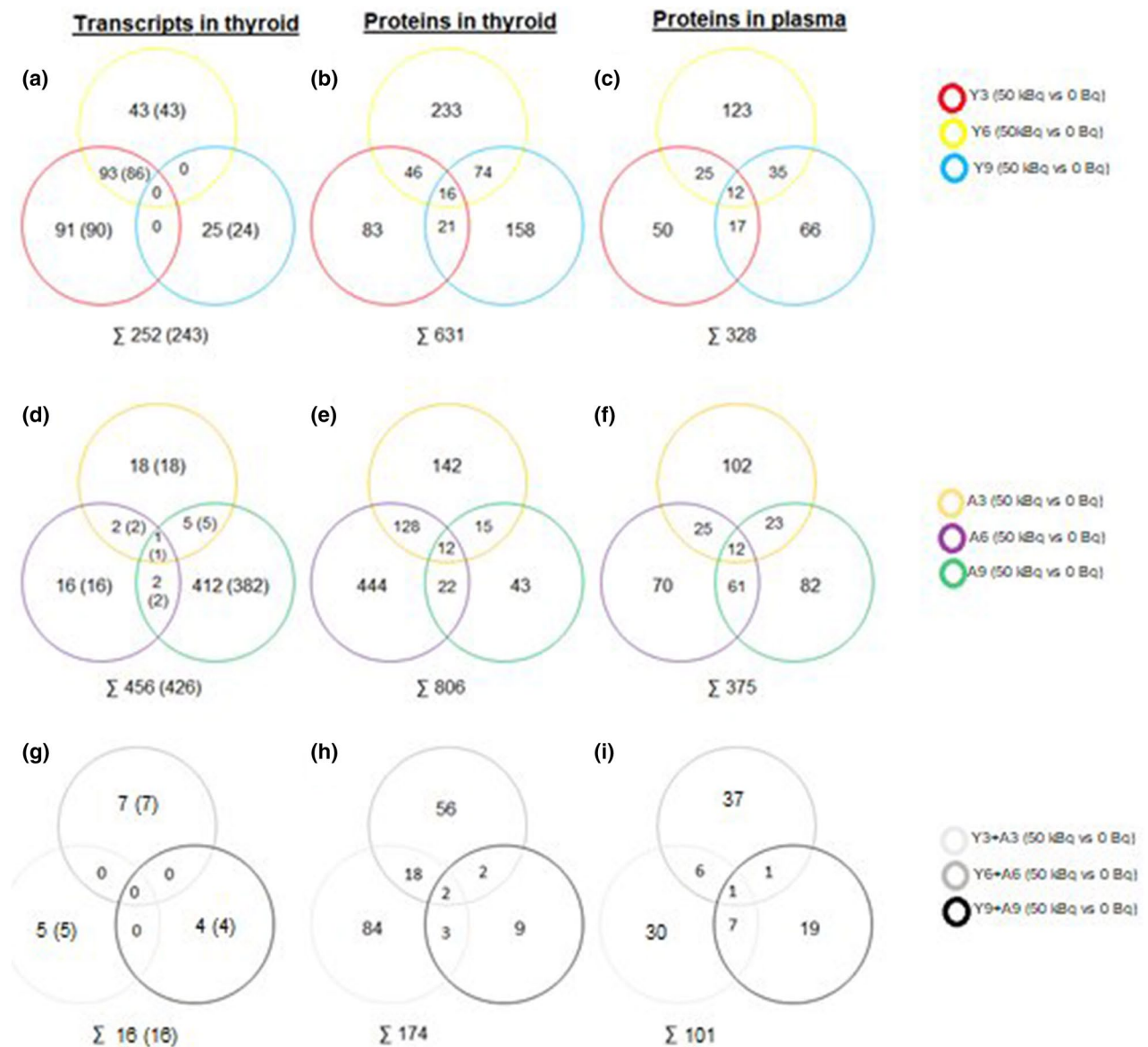


Figure 1. A schematic illustration of the distribution of statistically significant transcripts and proteins in rats exposed to ^{131}I . Venn diagrams displaying the number of (a, d, g) transcripts identified in thyroid tissue (b, e, h) proteins identified in thyroid tissue and (c, f, i) proteins identified in plasma. Panels (a–c) and (d–f) represent young (Y) rats and adult (A) rats, respectively, while (g–i) show transcripts or proteins identified at three, six or nine months after irradiation in both young and adult rats. When reporting number on transcripts, the number of related genes id given in parenthesis. In legends, Y denotes young and A adult rats, and the figure gives the number of months after injection of ^{131}I .

Table S2). Among the identified proteins with uniform expression, nineteen were found in the A3 + A6 groups and six in the A6 + A9 groups (Fig. 2). Totally, 12 proteins (CPQ, DPYSL2, EIF3J, GOT1, HSPB6, HMG2, KRT1, KRT13, MYBPC1, PTH, PVALB, and RPLP2) were detected in all three adult groups (Fig. 3). The HSPB6 protein showed increased expression levels for all groups in adult rat thyroid tissue.

The LQ-MS/MS analysis identified 375 differentially expressed proteins in plasma from irradiated adult rats, of which 70, 102, and 82 proteins were unique for the A3, A6, and A9 groups, respectively (Fig. 1f, Supplementary Table S7). The 20 proteins with the highest differential expression levels are presented in Fig. 2. None of these proteins was associated with thyroid tissue according to HPA. In total, 109 regulated proteins were identified in two of the groups, where 19 proteins with uniform expression were found in the A3 + A6 groups and two in the A6 + A9 groups (Fig. 2). Twelve regulated proteins were commonly detected in all adult groups (HIST1H1E, MCPT1, FN1, HINT1, APOC4, eEFEA1, HIST1H4B, HSP90B1, F9, MYL6, LBP, and FKBP1A; Fig. 3).

Common effects irrespective of age and time. sixteen regulated RNA transcripts (16 genes) in thyroid, and 174 and 101 proteins in thyroid and plasma, respectively, were found in both young and adult rats for at least one of the three time points after ^{131}I injection (Fig. 1g–i). Two proteins in thyroid (KRT13 and PTH)

(a)

Y3			Y6			Y9			Y3+Y6				Y3+Y9		Y6+Y9	
transc(th)	prot(th)	prot(pl)	transc(th)	prot(th)	prot(pl)	transc(th)	prot(th)	prot(pl)	prot(th)		prot(pl)		prot(th)	prot(pl)	prot(th)	prot(pl)
ALDH3A1	SPRR1A		<i>Adh7</i>	BPFA1	PSBPC2	<i>Col10a1</i>	FASN	CPS1	A1B	GSTA1	CA1	RNASE4	HBA1	CA1	COMP	UBE2N
CNN1	DIEXF		<i>Krt15</i>	PLP2	CAPZA1	<i>Col10a1</i>	IKBKB	FAM129A	A1M	HDLBP	CFL1	APOH	HBB	TGM3	OCM	CAT
PF4	CSPG4		<i>Bpifa5</i>	DAP	CAP1	<i>Mafn1</i>	DDR1	ACP1	ACADSB	HP	PFN1	VIM	HRSP12	HAGH	APQA1	GSTA4
DPYSL3	CYBSA		<i>LOC6833313</i>	COX6A2	CAPZA2	<i>Muc16</i>	PRPSAP2	TPP2	ACOT2	IGFALS	EML2	LBP		PF4	APOA2	BLMH
CLEC2D11	SPTBN2		<i>Lce11</i>	CRAT	PPIA	<i>Acan</i>	RAB11B	GLO1	AP1B1	PTH3	CAPN1	Uncharacterized protein C10orf88 homolog		UBB	APOD	SPR
DNAJB6	ATP6V0C		<i>Kihl14</i>	DNAJC27	UBE2V2	<i>Chad</i>	Ester hydrolase C11orf54	PLCB4	C4	BCKDHA	LONP1			PPB	NPM1	GDA
SERPINF1A	VWF		<i>RGD1563692</i>	GNB2	GYG1	<i>Cd300lg</i>	Scgb1a1	homolog	CA1	MUG1	CALM1	RT1-AW2		PPB	LTA4H	EEF2K
AKT1	SLC25A5		<i>RGD1565410</i>	MAOA	UPF0887 protein C20orf127	<i>Col2a1</i>	APRT	GPX1	CA2	MYPBH	RGN			DMBT1	PROC	HIST1H4B
COPB1	SELL		<i>Trpm6</i>	CHDH	MYH6	<i>RGD1305045</i>	GMFB	ATIC	CAMK1	PCCA	PCCB	GSTA2		RT1-AW2	LMNA	PEPD
RBM10	IL1R2		<i>Pglyrp3b</i>	MYH6	PCSK9	<i>Adra1b</i>	TUBA8	TAO3K	CES1C	PCCB	GSTA2			EEF1A1	EEF1A1	CA1
UPF0235 protein C15orf40 homolog			<i>Kik12</i>	MYH3	PCSK9	<i>Dra1b</i>	TUBA8	TAO3K	CES1D	PTPN11	SOD1			JUP	JUP	CA2
HSPH1			<i>RT1-CE5</i>	GNB1	HABP2	<i>Ddb</i>	NUP54	Urinary protein 1	CNP	SERPND1	PVALB			DSG4	DSG4	SKAP2
STRN3			<i>Fam163a</i>	TMX2	PSMA5	<i>Fam65c</i>	GPT	GBB	CSAD	TMED7	AKR1D1			F7	F7	BLVRA
ENPP1			<i>Slc4a9</i>	RTN1	NOVA1	<i>Entpd2</i>	Histone H2B type 1	FTH1	DNAAF2	TUBB2A	FTL1			PRDX4	PRDX4	PVALB
STAMBP			<i>Trex2</i>	LGALS3	F2	<i>Gdf15</i>	PYURF	ATP2A3	EEF1A1	TUBB3	ADH1			FTL1	FTL1	CSRFP
ESP			<i>Dcdc2</i>	MYH8	TGFB1	<i>Col9a2</i>	DHRS4	SPP1	ETFDH	FABP3	LYN			HRSP12	HRSP12	SPNK3
AP2B1			<i>Vcsa1</i>	LRRCS9	INHBC	<i>Ceacam16</i>	NOLC1	RAP2B	ETFDH	FABP3	LYN			HRSP12	HRSP12	ATPSA1
RAB7A			<i>Lilrb3l</i>	MYH11	PCYOX1	<i>LOC102546805</i>	TOR1AIP1	CANX	FGF	PLEC	RGS18			RGS18	RGS18	CYCS
ITGB4			<i>LOC685560</i>	PCSK1N	PSAP	<i>Glis1</i>	GNPMB	PRKCA	GSS	RAD23B	ATRNL			ATRNL	ATRNL	CTBS
GSTA4				SCG5	LIPC		SCN1B	BID								
				GSTM5	PSMA7		NCL	SAE1								
				PSMA7												

(b)

A3			A6			A9			A3+A6			A3+A9			A6+A9		
transc(th)	prot(th)	prot(pl)	transc(th)	prot(th)	prot(pl)	transc(th)	prot(th)	prot(pl)	prot(th)		prot(pl)		transc(th)	prot(th)	prot(pl)	prot(th)	prot(pl)
<i>Mup4</i>	MED22	G6PDX	<i>LOC100360165</i>	RALA	DHTKD1	<i>Myh6</i>	CALD1	HNRNPA2B1	<i>Vegfb</i>	ADA	DPP3	<i>Gcx</i>	EF3J	TPR	ACTN1	FKBP1A	
<i>Pax4</i>	YIPF3	ILK	<i>Bmp8a</i>	TUBB4B	ALDH7A1	<i>Myh7</i>	PSME2	HNRNPK	<i>Kik1c9</i>	CACNG6	CP		MCM8	F9	PIF	NF1	
<i>LOC102556288</i>	Uncharacterized protein C15orf40 homolog	MYH10	<i>Wfdc10</i>	RPS10	TG	<i>Myh2</i>	CRELD1	PGAM1		CAPRN1	PEPD		BN1	CFL1	PRKAR2A		
<i>Miox</i>	Uncharacterized protein C15orf40 homolog	MYH10	<i>Upk1b</i>	DNM1L	GLYCAM1	<i>Alah1a7</i>	TMOD1	ACTR1A		CASQ2	PSMB8		PVALB	ENPEP	S100A10		
<i>Hao2</i>	Uncharacterized protein C15orf40 homolog	CALR	<i>Fh1</i>	USO1	EPHX1	<i>Tnnt1</i>	BGN	DNM2		COMP	LALBA		PTMA	ACTB	HMGB1		
<i>Umod</i>	Uncharacterized protein C15orf40 homolog	MINPP1	<i>Npw</i>	TFAM	ICAM1	<i>Tnnt1</i>	HSPB7	ATP5B		CSR3	HIST1H1E		MYL2	RAB11A	TG		
<i>LOC360228</i>	Uncharacterized protein C15orf40 homolog	MINPP1	<i>Kik1c4</i>	SCN4B	XYLB	<i>Kihl30</i>	FKBP1A	ACPP		ECM1	BASP1		MYL3	YWHAZ			
<i>Slc7a13</i>	Uncharacterized protein C15orf40 homolog	MINPP1	<i>Gk</i>	GLO1	PECAM1	<i>Tnnc1</i>	GSTA5	MSN		FABP5	CKM		HSPB6	YWHAQ			
	Uncharacterized protein C15orf40 homolog	MINPP1	<i>Gh1</i>	DCTN2	MTHFD1	<i>Lbx1</i>	BCAM	HAL		FMOD	ENO3		SRSF5	TUBB2A			
	Uncharacterized protein C15orf40 homolog	MINPP1	<i>C4bpa</i>	HIST1H1E	ASS1	<i>Myh2</i>	RPS28	YWHAZ		KRT14	HIST1H4B		KRT6A	ACTR3			
	Uncharacterized protein C15orf40 homolog	MINPP1	<i>Slc20a1</i>	LZC	ECM1	<i>Sh3rf2</i>	LMBN1	HSP90AB1		KRT15	EEF1A1		TPPP3	TUBA4A			
	Uncharacterized protein C15orf40 homolog	MINPP1		UCHL1	CCL6	<i>Rbm20</i>	EIF5A	LRRCS9		KRT4	MCPT1		KRT1	PDIA6			
	Uncharacterized protein C15orf40 homolog	MINPP1		LMAN1	CRYAB	<i>Myh2</i>	ST13	TUBB4B		LGALS7	ADH1		KRT5	CRK			
	Uncharacterized protein C15orf40 homolog	MINPP1		NEFM	APOB	<i>Neu2</i>	NDUFV2	EIF4A2		SCGB1A1	HP		WFDC2	MYL6			
	Uncharacterized protein C15orf40 homolog	MINPP1		CST3	SNED1	<i>LOC100911353</i>	CMBL	KPNB1		AKR1A1	APOC4		NDRG2	HSP90B1			
	Uncharacterized protein C15orf40 homolog	MINPP1		THRSP	APOA5	<i>Fsd2</i>	PRPH	ARF5		APOA2	CSR3		SMPX	TUBA1C			
	Uncharacterized protein C15orf40 homolog	MINPP1		H2AFZ	ABCC6	<i>En1</i>	ATP5H	HSPA8		PLIN1	HINT1		COL1A1	CLIC1			
	Uncharacterized protein C15orf40 homolog	MINPP1		GGT5	CPB2	<i>Fbxo40</i>	COQ9	SPTAN1		PYGM	DAK		IGH-1A	DBNL			
	Uncharacterized protein C15orf40 homolog	MINPP1		AGA	OLFM1	<i>Asb14</i>	PRELP	TPM2		RPN1	FN1		CA2	BHMT			
	Uncharacterized protein C15orf40 homolog	MINPP1		PODXL	CSR1	<i>Prkag3</i>	HINT1	MAK					DPYSL2	PVALB			
	Uncharacterized protein C15orf40 homolog	MINPP1											HIST1H4B	PTMS			
	Uncharacterized protein C15orf40 homolog	MINPP1											H3F3B	GSTA2			
	Uncharacterized protein C15orf40 homolog	MINPP1											MPST	ARG1			
	Uncharacterized protein C15orf40 homolog	MINPP1											ARHGDI3	DBI			
	Uncharacterized protein C15orf40 homolog	MINPP1											MYBPC1	CTH			
	Uncharacterized protein C15orf40 homolog	MINPP1											CPQ	FAH			
	Uncharacterized protein C15orf40 homolog	MINPP1												HSPE1			
	Uncharacterized protein C15orf40 homolog	MINPP1												HRSP12			
	Uncharacterized protein C15orf40 homolog	MINPP1												DDT			
	Uncharacterized protein C15orf40 homolog	MINPP1												RGN			
	Uncharacterized protein C15orf40 homolog	MINPP1												RAD23B			
	Uncharacterized protein C15orf40 homolog	MINPP1												DPEP2			
	Uncharacterized protein C15orf40 homolog	MINPP1												Uncharacterized protein C10orf88 homolog			
	Uncharacterized protein C15orf40 homolog	MINPP1												LBP			

Decreased expression levels
 Increased expression levels

Figure 2. The 20 transcripts and proteins with highest expression levels in thyroid tissue, and plasma for (a) young and (b) adult rats exposed to ¹³¹I. Red or blue colour represents increased or decreased expression levels, respectively Y stands for young, A for adult, transc(th) for transcripts in thyroid tissue, prot(th) for proteins in thyroid and prot(pl) for proteins in plasma.

and one protein in plasma (eEF1A1), but no RNA transcript in thyroid were identified at all time points (Fig. 3). KRT13 protein expression was increased in the Y6, Y9, A3, and A6 groups and decreased in the Y3 and A9 groups. PTH protein expression was elevated in the Y9 and A9 groups and reduced in the remaining four groups. The expression of eEF1A1 was increased for Y3, Y9, and A9 and decreased for Y6, A3, and A6 (Fig. 3).

Of the 20 most differentially expressed RNA transcripts and proteins in rats irrespective of age the *Pth* and *Krt13* genes and the PTH, and KRT13 proteins were found in thyroid tissue for at least one time point (Supplementary Tables S8–Tables S10).

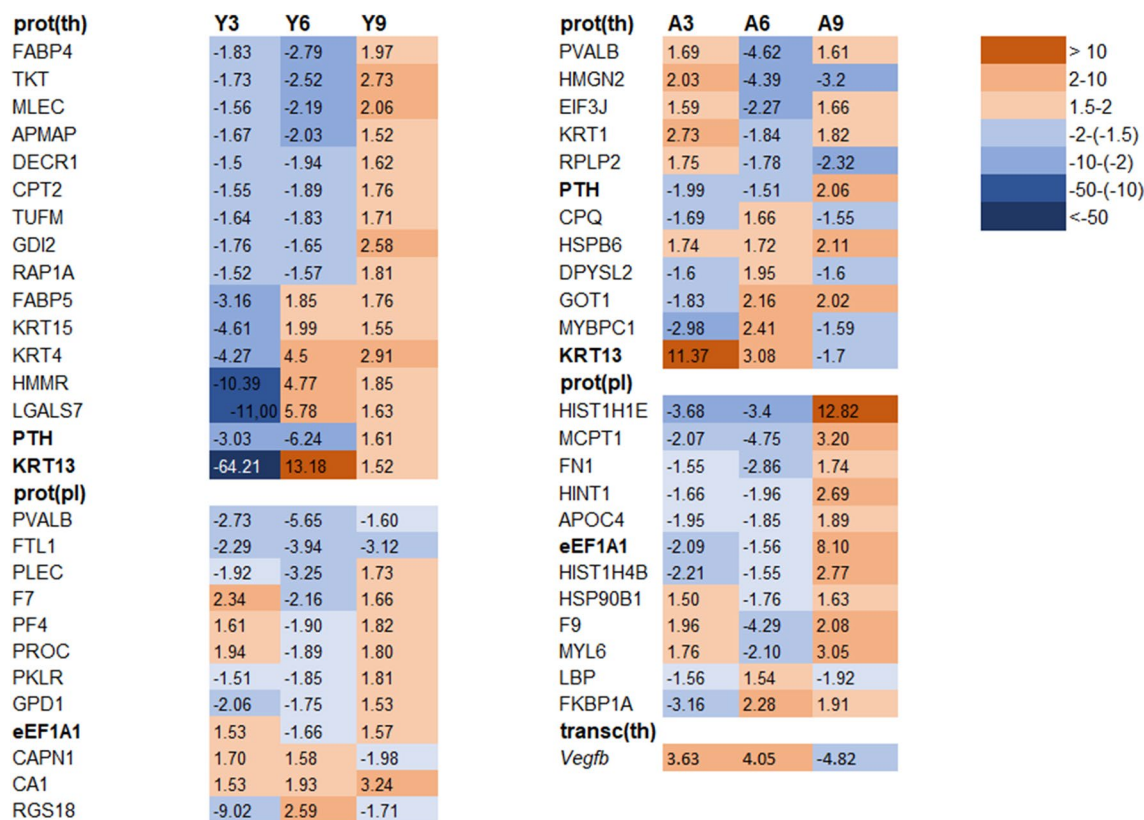


Figure 3. Common transcripts and proteins in young and adult rats at all three time points, respectively. The proteins marked with bold are common for both young and adult individuals. Transcripts in thyroid transc(th), protein in thyroid prot(th) and proteins in plasma prot(pl) are represented and Y = young and A = adult. Red represents increased expression, and blue represents decreased expression. A darker colour represents higher/lower expression.

Age-related effects. In total 181, 155, and 441 RNA transcripts were found differentially expressed when comparing young and adult rats 3, 6 and 9 months after ^{131}I exposure (Fig. 4a–c), of which 160 and 17, 129 and 19, and 22 and 416 transcripts were uniquely regulated in Y3 and A3, Y6 and A6, and Y9 and A9 groups, respectively. In total, 167, 589 and 345 proteins in thyroid tissue were identified after 3, 6 and 9 months, respectively (Fig. 4d–f), including 59 and 498, 292 and 219, and 253 and 76 uniquely regulated proteins in Y3 and A3, Y6 and A6, and Y9 and A9 groups, respectively. In total, 227, 311 and 280 proteins in plasma were identified after 3, 6 and 9 months, respectively (Fig. 4g–i), of which 59 and 123, 149 and 116, and 102 and 150 were uniquely regulated in Y3 and A3, Y6 and A6, and Y9 and A9 groups, respectively.

Time-related effects irrespective of age. The 16 regulated RNA transcripts (16 genes) in thyroid were unique for only one time point; 5 (*Col17a1*, *Dmkn*, *Sbsn*, *Sipi* and *Sprr1a*), 7 (*Klklc2*, *Klklc9*, *Krt13*, *Lgals7*, *RGD1562234*, *Sln*, and *Vegfb*) and 4 (*Ankrd2*, *Afp*, *Fam65c* and *Rt1-Bb*) at 3, 6 and 9 months, respectively, when evaluating data for young and adult rats together (Figs. 1g, and 5). The number of regulated unique proteins in thyroid for each time point were 84, 56, and 9 after 3, 6 and 9 months, respectively (Figs. 1h and 5). Corresponding numbers of unique proteins in plasma were 30, 37 and 19 (Figs. 1i and 5). Moreover, KRT13 and PTH proteins in thyroid and eEF1A1 protein in plasma were identified in all age groups at the three time points (Fig. 3).

In a separate analysis at each time point, five, seven and four transcripts were in common for Y3 + A3, Y6 + A6 and Y9 + A9 groups, respectively (Fig. 4). Furthermore, 107, 78 and 16 proteins were in common for Y3 + A3, Y6 + A6 and Y9 + A9 groups, respectively. The number of proteins in common for Y3 + A3, Y6 + A6 and Y9 + A9 groups were 44, 46 and 28, respectively.

Hormone levels in plasma. Nine months after exposure the plasma levels of T3 was about twice higher in exposed rats ($162 \pm 1(\text{SD})$ in young and $166 \pm 2(\text{SD})$ in adult rats) compared with controls ($80 \pm 1(\text{SD})$ and $79 \pm 3(\text{SD})$, respectively).

Corresponding values for T4 were $43 \pm 1(\text{SD})$, $42 \pm 3(\text{SD})$, $39 \pm 5(\text{SD})$ and $46 \pm 2(\text{SD})$, respectively. The TSH level in all samples were lower than the detection limit of the kit.

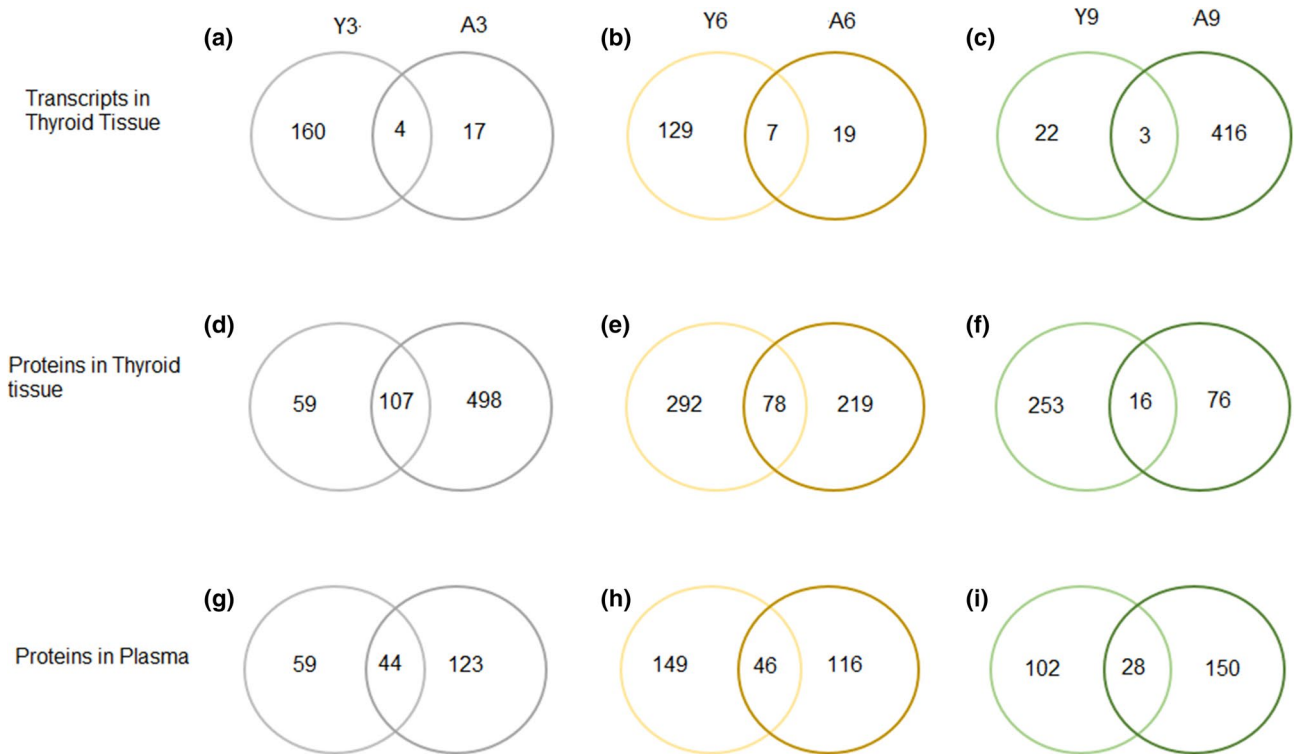


Figure 4. Venn diagram of age-related transcripts in thyroid and proteins in thyroid and plasma. Panels (a–c) display common and unique transcripts in thyroid for Y3 vs. A3, Y6 vs. A6 and Y9 vs. A9, respectively. (d–f) displays common and unique proteins in thyroid for Y3 vs. A3, Y6 vs. A6 and Y9 vs. A9, respectively. (g–i) displays common and unique proteins in plasma for Y3 vs. A3, Y6 vs. A6 and Y9 vs. A9, respectively. Y represents young rats and A represents adult rats, and the following numbers indicates the number of months after ^{131}I administration.

Histological evaluation of rat thyroid tissue. Individual thyroid tissue samples were morphologically evaluated for each rat. In the young exposed rats 3/6, and in adult exposed rats 1/6 had neoplastic changes, respectively. In the young control group 4/6 and in the adult control group 3/6 had neoplastic changes.

Pathway analysis using GO term annotation and IPA software. Significantly enriched GO terms included metabolism and cellular integrity. The distribution of enriched GO terms in the 18 groups were evaluated and displayed in a heat map (Fig. 6). Overrepresented GO terms included cell cycle and differentiation and metabolism, while DNA integrity and gene expression integrity were detected to a lower extent. Stress response and cell communication were enriched in the transcriptomic data, but less so in the proteomic data (thyroid and plasma). The associated GO terms for the 16 commonly regulated proteins in young rat thyroids were mainly associated with metabolism, signal transduction, physicochemical environment, and cell death. The 12 thyroid tissue proteins obtained in adult rats were primarily associated with metabolism, oxidative stress, immune system, inflammation, differentiation and aging. For the 12 significant proteins in plasma for young rats, associated GO terms included cytoskeleton & motility, general and protein metabolism, RNA processing, signal transduction, and supramolecular maintenance. The GO terms for the corresponding 12 proteins in plasma from adults included intercellular signalling, RNA processing, signal transduction, supramolecular maintenance and transcription. Several proteins were commonly detected in both young and adult rats. The PTH associated GO terms included e.g. metabolism, proteins and signal transduction, while cytoskeleton and motility, ontogenesis, also stress response and supramolecular maintenance were related to KRT13, and cell death and apoptosis for eEF1A1. Furthermore, the *Vegfb* transcript was only detected in adult rats and was associated with several GO terms, e.g. apoptotic cell death, cell cycle regulation and immune response.

Up-stream regulator analysis with IPA software. Significantly expressed RNA transcripts and proteins were used for a group-wise analysis of canonical pathways and up-stream regulators to evaluate radiation-induced cellular mechanisms detected in thyroid tissue and plasma (Supplementary Table S11 and Table 1). The majority of the canonical pathways were detected in one group. Some canonical pathways were more prevalent than others, e.g. Ephrin signalling (down-regulated Y3, Y6, A3, and up-regulated in Y9), Integrin signalling (up-regulated for Y9 and A3, and down-regulated for Y3, Y6 and A3) and Paxillin signalling (up-regulated Y6, Y9, A3 and A6). RhoA related signalling pathways were seen primarily in young individuals, but also for the A3 group (up-regulated for all except for two pathways in Y3). Only three upstream regulators were detected (Table 1). PPARG was identified as an upstream regulator for Y6 and A3 (down-regulated), and for Y9 and A6

Unique transc(th)			Common prot(th)			Unique prot(th)			Common prot(pl)			Unique prot(pl)				
Y3+A3	Y6+A6	Y9+A9	Y3+A3	Y6+A6	Y9+A9	Y3+A3	Y6+A6	Y9+A9	Y3+A3	Y6+A6	Y9+A9	Y3+A3	Y6+A6	Y9+A9		
<i>Col17a1</i>	<i>Klk1c2</i>	<i>Fam65c</i>	PTH	PTH	PTH	A1I3	MAP2K5	APOA2	PPF	HIST1H4B	EEF1A1	EEF1A1	EEF1A1	ARG1	APOC4	COTL1
<i>Dmkn</i>	<i>Klk1c9</i>	<i>Afp</i>	KRT13	KRT13	KRT13	ACADSB	MLEC	CHGA	PRDX3	HMGB1	ADH1	ADH1		ATRN	BASP1	CPQ
<i>Sbsn</i>	<i>Krt13</i>	<i>Ankrd2</i>	A1M	A1M		ACOT2	MVP	COQ7	RPS7	GOT1	AKR1D1	AKR1D1		BHMT	CKB	LYN
<i>Slpi</i>	<i>Lgals7</i>	<i>RT1-Bb</i>	C4	C4		ACTR1A	MYBPH	HAGH	SELENBP1	GPD1	GPD1	GPD1		CTH	CLTC	PDE5A
<i>Sprra1</i>	<i>RGD1562234</i>		CA1	CA1		ACTR2	PA2G4	PLN1	SUCLG1	PVALB	LBP	LBP		DAK	CSR3P	PRDX5
	<i>Sln</i>		CES1D	CES1D		ALDH7A1	PABPC1	PYGM	TRAP1	SMPX	CKM	CKM		DBI	ENO3	SERP1B10
	<i>Vegfb</i>		ETFDH	ETFDH		ANXA8	PCCA	RPN1	UQCRC2	USMG5	MCPT1	MCPT1		DDT	F10	ACLY
			FABP4	FABP4		AP1B1	PCCB	SCG3	VDAC1	DSTN	HRSP12		HRSP12	FABP3	F12	ESD
			FGB	FGB		APCS	PDXK	CASQ2	ENSA	ITCO2	PVALB		PVALB	FAH	FCN1	GPS
			MUG1	MUG1		APMAP	PGD	COMP	KRT10					GSTA2	FN1	Histone
			RAP1A	RAP1A		ARF3	PLG	HMMR	KRT2					LGALS1	HINT1	H2A type 3
			TKT	TKT		ARPC1B	POR	HSPB6	MARCKSL1					RGS18	HIST1H1E	LTA4H
			TUFM	TUFM		BCKDHA	PRDX2	RT1-AW2	NUCKS1					RGS18	HIST1H4B	NPM1
			ADA	ADA		CA2	PTGR1	ACADL	TNNT1					RGN	HP	ATPSA1
			CSR3P	CSR3P		CA5B	PTPN11	ACADM						VIM	LTBP1	CALD1
			FABP5	FABP5		CAP1	RAB5A	ACADS						ARPC2	MASP1	DLGAP4
			KRT14	KRT14		CAT	RAB6A	ACADVL						CFL1	MUG2	CLIP2
			KRT15	KRT15		CD47	RALB	ACO2						EML2	PROS1	AUNP
			KRT4	KRT4		CES1C	SEC11A	ADCK3						PFN1	SERP1A11	BAAT
			LGALS7	LGALS7		CNP	SEPT2	ALDH2						PLCG2	SERP1E2	SKAP2
			HRSP12		HRSP12	COL1A2	SEPT7	ALDH6A1						RLC-A	SRGN	
			CPQ		CPQ	CPT2	SERPIND1	ALDH9A1						SDPR	CA2	
			DPYSL2		DPYSL2	CRYL1	SERP1NH1	ARCN1						TES	CP	
					MYBPC1	MYBPC1	CSAD	SLC25A16	ATP2A1					ENPEP	DMBT1	
					HMG2	HMG2	DCPS	SMC3	ATPSA1					ANXA1	DPP3	
						DECR1	TF	C3						ANXA2	FDPS	
						DNAAF2	TMED7	CS						DSG4	PEPD	
						DNAJA1	TUBA1C	DLAT						EZR	PSMB8	
						EEF1A1	TUBB5	DLD						NRF1	RNH1	
						END2	TWF1	ECDC1						UBB	SPR	
						FAM213A	WDR1	ECI2							ALDH2	
						GD2	XPNPEP1	EEF1A2							LALBA	
						GSN	ATPF1	EIF4A2							PLEC	
						GSS	CACNG6	GLUL							PSMB4	
						GSTA1	KRT5	GOT2							ACTN1	
						GSTT2	LYPD3	GPX3							ALOX12	
						HNRNP1A1	MYL3	IVD							CAPN1	
						HP	NRGN	Major urinary protein							FLNC	
						IGFALS	OBP1F	MYH9								
						IGG-2A	PLET1	OXCT1								
						ITIH3	S100A4	PDH1A								
						LONP1	Vomeromodulin (Fragment)	PHB2								

Decreased expression levels (young and adult rats)
 Increased expression levels (young and adult rats)
 Decreased expression levels young rats and increased expression levels adult rats
 Increased expression levels young rats and decreased expression levels adult rats

Figure 5. Transcripts and proteins differentially regulated in both young and adult rats three, six and nine months after ¹³¹I injection. Data are presented separately for common proteins (differentially regulated at two or three time-points) and unique transcripts or proteins (differentially regulated at one time-point only). Blue colour represents decreased and red colour increased expression level, yellow represents decreased expression in young and increased expression in adults, white represents decreased expression in young and increased expression in adult individuals.

(up-regulated) groups. In addition, VCAN was present for, Y6 and A9 (up-regulated), and A6 (down-regulated). NFkB was identified in the Y9 group.

Discussion

The current work was designed to expose young and adult rats with ¹³¹I in order to obtain an absorbed dose to the thyroid of 100 mGy, which is in the same range as children and adults received due to the Chernobyl accident. We also chose to relate our findings not only with thyroid cancer, but also effects on the thyroid function.

In the present study, radiation-induced effects on the proteome and transcriptome expression patterns in thyroid and plasma varied depending on the age of exposed rats and time after exposure. No general trend in differences in number of differentially expressed RNA transcripts and proteins was found between adult and young rats or with time after exposure. Four potential age- and time-dependent biomarkers showed unidirectional expression (up- or down-regulation) levels for all three time points, including three in young rats (CA1, FTL1, and PVALB proteins in plasma) and in adults one protein in thyroid tissue (HSPB6). Of these, only CA1 varied monotonously with time. Three biomarker candidates, depending on time and independent of age, were found, however, with varying direction of expression: two proteins in thyroid tissue (KRT13 and PTH) and one protein in plasma (eEF1A1). The PTH protein had either decreased (3 and 6 months) or increased (9 month) expression levels for both young and adult individuals at the same time point. No single biomarker candidate related to age irrespective of time after exposure was identified. Consequently, a panel of 20 proteins with the highest up-regulation in plasma, related to age and irrespective of time after exposure, is proposed for each age group (young and adult) (Table 2). The *Vegfb* transcript was identified in adults at 3 (up-regulated), 6 (up-regulated), and 9 months (down-regulated) after exposure and is suggested as a biomarker candidate that is related to thyroid function. Furthermore, several of the identified transcripts and proteins, correlated to age at a certain time-point, have previously been related to thyroid diseases. Of these, *Ada* (Y3), *Tgm3* (Y3 and Y6), *Vegfb* (A3 and A9) and *Pth* (A9) genes in thyroid tissue, *RPN2* (Y9 and A3), *DLD* (A3) and *ACADL* (A3) in thyroid tissue and *PVALB* (Y6) in plasma were previously proposed as long-term biomarker candidates in our previous study²⁴.

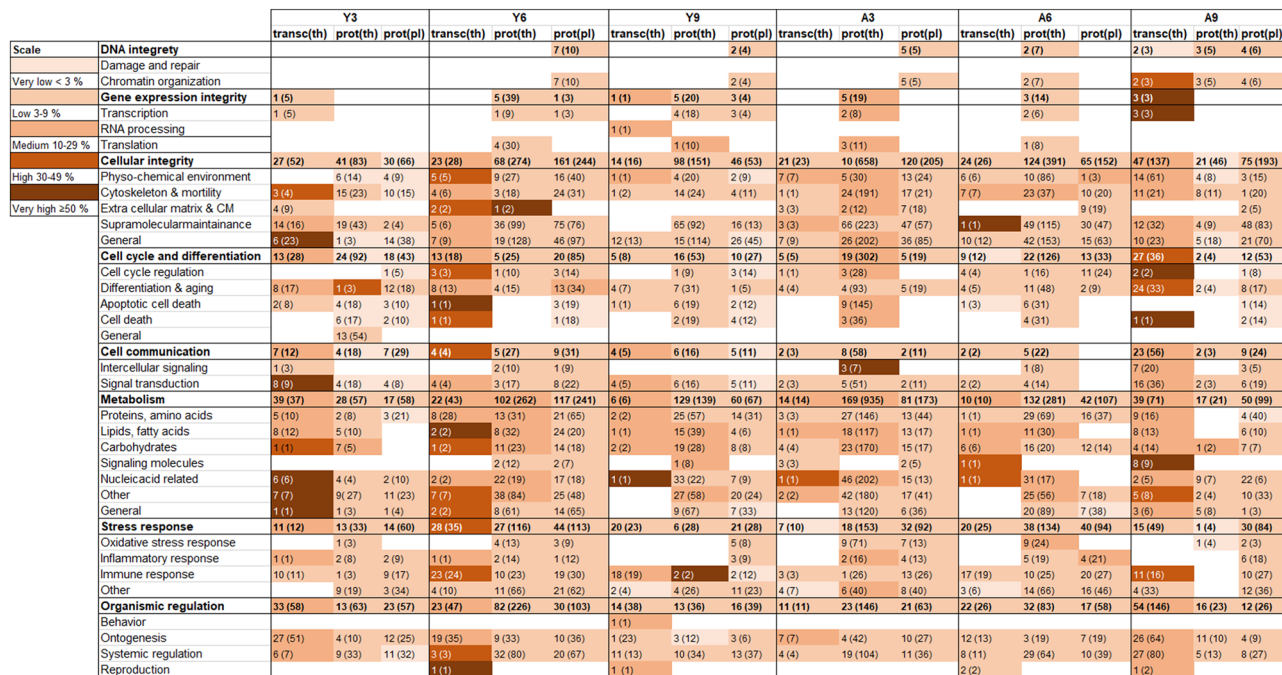


Figure 6. Heat map of transcript and protein response in thyroid tissue and plasma, showing enriched biological processes categorised by GO terms for cellular function. The heat map was constructed from transcripts in thyroid transc(th) and proteins in thyroid prot(th) and proteins in plasma prot(pl) with significant levels by using categorisation of enriched biological processes based on GO ancestor charts. The percentage of scored vs filtered transcripts or proteins is displayed by very light orange, light orange, orange, dark orange and brown representing the percentage very low < 3%, low 3–9%, medium 10–29%, high 30–49% and very high ≥ 50%, respectively. The number of scored transcripts or proteins are displayed, and the total number of associated GO terms are presented in parentheses. Y = young, A = adult.

Upstream regulators	p	z	Target molecules in dataset
Y6			
Proteins in thyroid			
PPARG	5.2×10^{-14}	-3.1	ACADL, ACADS, ACLY, ACSL1, CD36, CS, DLAT, FABP4, HADHA, HADHB, PC, Slc25a1, SLC25A20, TAGLN
Proteins in plasma			
VCAN	6.4×10^{-3}	2.2	APOE, LBP, RNASE4, TGFB1, VCL
Y9			
Proteins in thyroid			
PPARG	4.8×10^{-10}	3.1	FABP5, KRT19, Ldha/RGD1562690, SOD2
NFkB (complex)	3.6×10^{-2}	2.0	COL1A1
A3			
Proteins in thyroid			
PPARG	2.8×10^{-12}	-3.8	ACADL, ACADS, ACLY, ACSL1, CD36, CS, DLAT, FABP4, HADHA, HADHB, MDH1, MGLL, PC, Slc25a1, SLC25A20
A6			
Proteins in thyroid			
PPARG	6.3×10^{-5}	3.0	ACADL, ACADS, CS, DLAT, FABP4, MDH1
Proteins in plasma			
VCAN	4.4×10^{-4}	-2.4	ASS1, C1S, ICAM1, LBP, LGALS3, PAM
A9			
Proteins in plasma			
VCAN	2.3×10^{-2}	2.0	LBP, MSLN, PRDX5, RNASE4

Table 1. Upstream regulators for ¹³¹I exposure in young and adult rats from the IPA software analysis. Activated (z > 2.0) or inhibited (z < -2.0) signalling pathways, are presented.

Panel for young individuals				Panel for adult individuals			
Proteins	Y3	Y6	Y9	Proteins	A3	A6	A9
ACTA2		×		ANXA1			×
ACTB		×		CMPK1			×
ANXA1	×			DHTKD1		×	
CA1	×	×	×	EEF1A1			×
CA2		×	×	EZR			×
COPS4			×	HIST1H1E			×
CORO1A		×		HIST1H2BA			×
CPS1			×	Histone H2A type 3			×
DSG4	×		×	Histone H3.1			×
LGALS5			×	HNRNPA2B1			×
NPM1	×		×	HNRNPC			×
NRIF1	×			HNRNPK			×
PFN1	×	×		LMNA			×
PRDX4	×		×	NPM1			×
PSBPC2		×		NRIF1			×
RGS18		×		PGAM1			×
RT1-AW2	×	×		PIGR		×	
SPRR1A	×			PPP1R7		×	
TPM4		×		PRDX4			×
XK	×			VCP			×

Table 2. Panels of biomarker candidates in plasma for ^{131}I exposure of young and adult individuals, respectively. The panel consists of the 20 proteins with the highest increased expression for each age group.

In the present investigation, several types of biomarkers could be identified: (a) biomarkers dependent on age and time after exposure, (b) time-dependent biomarkers independent of age (c) age-dependent biomarkers but independent of time after exposure, and (d) biomarkers independent of age and time after exposure (related to exposure or not). Ideally, biomarker candidates should be related to effects on thyroid tissue e.g. thyroid function and thyroid carcinogenesis. Furthermore, biomarker candidates with uniformly increased or decreased expression levels are technically easier to evaluate at any time point. It is also important that the biomarkers have relatively high differential expression as an effect of irradiation compared with noise due to small individual differences. When no single RNA transcript or protein can reflect a defined property (such as absorbed dose or time after exposure), a panel of biomarkers with expression patterns depending on these properties may be more appropriate²⁵. An optimal biomarker panel should include up-regulated markers, to be able to easily distinguish exposed from non-exposed individuals. It would also be preferable if the biomarker candidates are detectable in blood samples, which are less invasive than tissue biopsies.

Four age- and time-dependent biomarker candidates with unidirectional expression were proposed, i.e. the CA1 (up-regulated), FTL1 (down-regulated), and PVALB (down-regulated) proteins were identified in plasma for young rats, and the HSPB6 (up-regulated) protein was identified in adult rat thyroid tissue. The CA1 is an enzyme involved in several biological processes e.g. respiration, bone resorption, saliva and gastric acid²⁶. A previous study found low CA1 levels in erythrocytes from hyperthyroid patients and proposed CA1 as a biomarker for different types of hyperthyroidism²⁷. The HSPB6 small heat shock protein maintains denatured proteins in a folding compartment state, and is involved in smooth muscle relaxation²⁶. The FTL1 protein is involved in iron storage in various tissues²⁶. The PVALB calcium ion-binding protein was previously proposed as a radiation biomarker candidate^{26,28}.

The KRT13, PTH, and eEF1A1 proteins were identified at all time points for young and adult individuals and were proposed as time-dependent, but age-independent biomarker candidates. The keratin (*KRT*) gene family encodes intermediate filaments involved in the internal cellular structure stabilisation and maintenance of cell shape²⁹. The parathyroid hormone (PTH) expression levels were consistent with time after exposure (three (up-regulated), six (up-regulated) and nine months (down-regulated)) for both young and adults. PTH regulates calcium and metabolism²⁶. *Krt13* (Y3 and A6) and *Pth* (A9) were identified among the 20 transcripts with the highest expression (Supplementary Table S8). The eukaryotic translation elongation factor A1 (eEF1A1) is a GTP-binding protein involved in cell growth, signal transduction, differentiation and apoptosis. Elevated eEF1A1 expression levels have been associated with increased cell proliferation and oncogenic transformation, and overexpression of mRNA was correlated with metastasis³⁰. Previously, the eEF1A1 protein was proposed as a biomarker for cellular senescence after radiation exposure in cancer cell lines³¹.

In the present study, no single age-dependent but time-independent biomarker candidate was found. Therefore, panels consisting of the top 20 differentially regulated proteins in plasma for young and adult rats are proposed. For young individuals, the panel consists of ACTA2, ACTB, ANXA1, CA1, CA2, COPS4, CORO1A, CPS1, DSG4, LGALS5, NPM1, NRIF1, PFN1, PRDX4, PSBPC2, RGS18, RT1-AW2, SPRR1A, TPM4, and XK. The

corresponding panel for adults contains ANXA1, CMPK1, DHTKD1, EEF1A1, EZR, HIST1H1E, HIST1H2BA, Histone H2A type 3, Histone H3.1, HNRNPA2B1, HNRNPC, HNRNPK, LMNA, NPM1, NRIF1, PGAM1, PIGR, PPP1R7, PRDX4, and VCP. Several of these biomarker candidates have previously been associated with thyroid diseases. Positive ACTA2 staining is common in PTCs from adults (27–54 years) and related to higher tumour grade and metastatic potential³². High CA1 expression is related to hyperthyroidism, as already discussed. Although CA2 gene expression was increased in our study, a previous study found decreased CA2 gene expression in young patients with PTC (15–39 years) but not in older PTC patients (> 40 years)³³. The methylation regulator HNRNPC was highly expressed in PTC and suggested as part of a molecular signature for PTC progression³⁴. The LMNA protein was one of the protein markers identified in a cluster for malignant thyroid cancer³⁵. The RT1-AW2 protein is involved in autoimmune thyroiditis²⁶. VCP is associated with the sodium iodine symporter (NIS), which is important for normal iodide transport into thyrocytes. Increased VCP expression is related to more aggressive cancer types and reduced iodide uptake, and VCP was suggested as a prognostic biomarker for FTC^{36,37}.

The vascular endothelial growth factor B (*Vegfb*) gene was the most interesting single biomarker candidate, related to thyroid function found in adults, and was up-regulated at 3 and 6 months and down-regulated at 9 months after exposure. VEGF plays a pivotal role in angiogenesis²⁶. Previously, *Vegfb* was also suggested as a biomarker for ¹³¹I exposure in mice²³. To be an ideal biomarker candidate for thyroid function and cancer induction, the RNA transcript or protein should be thyroid tissue related. The *Vegfb* gene is not thyroid tissue related, but TG protein is thyroid-specific and ACADL is involved in metabolic processes, and both were detected in young and adults. However, they were only detected in some of the groups and are therefore not proposed as biomarker candidates in the present study. Taken together, these findings indicate that irradiation has an effect on thyroid function, although effects may vary depending on age and time after exposure.

In the present study, the number of identified GO terms was highest for proteins in thyroid followed by proteins in plasma and RNA transcripts in thyroid. The RNA transcripts showed high correlation to associated GO terms. The enriched GO terms were metabolism and cellular integrity, with the subgroups nucleic acid related metabolism, and cytoskeleton and motility, respectively. High association with metabolism is interesting, since the thyroid hormones triiodothyronine (T3) and thyroxine (T4) play a major part in various metabolic processes. During hyperthyroidism, metabolism in the body is increased via increased T3 and T4 blood levels that results in reduced thyroid stimulating hormone (TSH) levels, and the opposite effect is seen for hypothyroidism³⁸. In a study on patients previously treated by external radiation therapy in the neck region (> 40 Gy), nearly half of the patients developed hypothyroidism within 9 months³⁹. In the present study T3 levels in plasma from exposed rats were twice higher, irrespective of age, than in corresponding controls after 9 months. The T4 levels were similar in all groups, while the TSH levels were low, indicating increased thyroid hormone production. In general, thyroid cancer usually do not give altered hormone levels. However, the histological analysis of the rat thyroids after 12 months demonstrated neoplastic cells in about half of the young animals and only one of the exposed adult rats. However, neoplastic cells were also found in some unexposed rats.

Canonical pathways related to signal transduction (Ephrin receptor signalling, Paxillin signalling, and integrin signalling) were predominantly seen in the young groups and A3 group. More specifically, the Ephrin receptor is involved in signal transduction and actin cytoskeleton, which controls cellular shape, adhesion and movement by regulation of the Rho GTPase family, including RhoA⁴⁰. Paxillin is a signal transduction adaptor protein that plays a crucial role in plasma membrane-associated adhesion and growth factor signalling, and regulating the actin cytoskeleton⁴¹. Integrin signalling is involved in the maintenance of the extracellular matrix and in the regulation of the cell cycle by activating several growth-promoting signalling pathways⁴². These findings suggest that radiation can induce cellular activation at low doses shortly after onset of exposure and is sustained over a period of time in young individuals, while the effect decreases with time in adult rats.

IPA analysis identified the upstream regulator PPARG in the majority of the groups (Y6, Y9, A3, and A6). PPARG belongs to the nuclear receptor family of transcription factors and is expressed at very low amounts in normal thyroid. PPARG is also involved in, e.g., regulation of tumour growth in several cancer forms²⁶. Elevated PPARG expression has been observed in PTC tissue⁴³. It is also commonly found as an oncoprotein PAX8/PPARG complex in FTC and are more prevalent in younger patients, and PAX8 and PPARG rearrangements may be important in PTC development^{36,37}. The transcription factor NFkB is known to be activated after radiation exposure, which may result in cancer development⁴⁴. Interestingly, NFkB was activated in the Y9 group only indicating a higher risk to induce cancer in young individuals.

No RNA transcript was in common for all young rats in the present study. This finding can have several explanations. One is that total RNA microarray analyses were performed on individual samples, while protein analyses used pooled protein samples for each group. Furthermore, the transcriptional response might be more rapid and/or inconsistent over time, and transcripts are frequently degraded quickly, while proteins are more stable over time. *Dbp* (Y9), was the only transcript identified in the present study as well as in our previous work^{22,28}. We also identified the following proteins both in the present study and in similar previous short-term studies on mice; in thyroid tissue: AOC3 (A3), ATP2A1 (Y6, Y9, A3, and A6), CPA3 (A3), PVALB (Y9, A3, A6 and A9), S100a8 (A3), S100a9 (A3), TNNI2 (Y9, A6), and TNNT3 (A6) and PTH (all groups), ACADL (Y6, A6; and in plasma: PVALB (Y3, Y6, Y9 and A3) and ENO3 (A6)^{20,21,23,28,45,46}. However, our former studies were short-term studies and some used another radionuclide, which might explain differences in results. In a previous review summarising more than 300 publications, 261 radiation responsive proteins were proposed⁴⁷. Of these proteins, 33 were also identified in the present study, including AFP, ALDH2, APOA1, APRT, BID, BLVRA CA1, CA2, CALR, CKM, CSTB, DDT, FABP5, GSS, FTH1, GGT1, GLO1, GPT, GPX1, HP, ICAM1, ILK, LYN, NPM1, PRDX2, PRDX3, PRDX5, PRDX6, PSMB4, SERPINB10, SPTAN1, TF, and VIM.

In comparison with adults, ¹³¹I irradiation of the thyroid is expected to have a profound effect on children, since children are more sensitive to radiation and showed higher incidence of thyroid cancer after the Chernobyl

accident. RNA microarray analyses of PTC tumours from primarily children exposed to radioactive fallout from the Chernobyl accident resulted in a plethora of suggested biomarkers, potentially due to the difficulty of using a representative control group (regarding age, dietary, geographical area, gender, etc.)^{9–15,48–58}. Furthermore, CLIP2 and TG were the only previously suggested biomarkers that were also identified in the present study^{11,12,16,53,54}. The CLIP2 protein was detected in plasma in the nine month groups, indicating that the time of exposure to the endpoint has a profound effect on whether certain genes or proteins can be detected. In contrast, the TG protein was differentially expressed in several of the groups, which is interesting since TG is involved in thyroid hormone production¹⁹.

In conclusion, the present study showed that radiation-induced effects depended on age, e.g. a higher number of regulated proteins were found in tissues from adult rats. Moreover, time after exposure affected the transcriptional and proteomic response, although no general trend was identified. Promising biomarkers were age- and time-dependent in young rats (CA1, FTL1 and PVALB, plasma) as well as in adult rats (HSPB6, thyroid tissue). The ¹³¹I exposure biomarker candidate (time-dependent but age-independent), PTH (in thyroid tissue), was detected in all six groups. Panels of biomarker candidates (age-dependent and time-independent) consisting of 20 proteins in plasma for young and adult rats, respectively, were proposed. Several of the identified biomarkers were among the previously identified specific genes involved in thyroid cancer and function. Furthermore, *Vegfb* (adults) was identified as a thyroid function biomarker candidate. However, these proposed biomarker candidates need to be further validated in human samples as a step towards clinical application or for radiation protection purposes. Altogether, none of these proposed transcripts or proteins can be considered as radiation-specific.

Methods

Experimental set-up. Forty healthy Sprague Dawley rats (Taconic, Denmark) were randomly divided into ten groups containing four individuals each. Rats in six groups were i.v. injected with 50 kBq ¹³¹I: rats in 3/6 groups were young, injected at 5 weeks of age, and the remaining 3/6 groups rats were adult, injected at seventeen weeks of age. The estimated absorbed dose to the thyroid was 0.1 Gy and 0.07 Gy for young and adult rats, respectively, assuming similar percentage uptake but smaller thyroid in young rats^{59,60}. The remaining four groups were age-matched untreated controls.

The animals were killed under pentobarbital (APL; Kungens kurva, Sweden) anaesthesia at three, six or nine months after study start. The number of control groups were optimised by simultaneously terminating the 3 months adult rats and the 6 months young rats, and the 6 months adult rats and the 9 months young rats, respectively. Individual thyroid samples were collected, flash-frozen in liquid nitrogen, and stored at -80°C until further analysis. Plasma samples were separated from individual blood samples, using heparin filled syringes and then flash-frozen in liquid nitrogen and stored at -80°C .

The animals were under daily supervision and had free access to standard rat chew and water. We did not record any weight loss or impaired general health condition in any of the rats. The experimental set-up was approved by the Ethical Committee on Animal Experiments in Gothenburg, Sweden (Permit Number: 146-2015). All methods were performed in accordance with the relevant guidelines and regulations and are reported in accordance with ARRIVE.

Gene expression analysis. Total RNA was extracted from flash-frozen thyroid samples using the RNeasy Lipid Tissue Mini Kit (Qiagen; Hilden, Germany). Microarray analysis was performed at the Bioinformatics and Expression Analysis Core Facility at Karolinska Institute (Stockholm, Sweden) using Agilent Sureprint G3 Rat GE 8×60 K microarrays (Agilent, Santa Clara, CA, USA). Nexus Expression 3.0 (BioDiscovery; El Segundo, CA, USA) was used to identify differentially expressed transcripts by comparing data from exposed and non-exposed individuals. The fold change cut-off value was set to 1.5 and the FDR adjusted p-value (Benjamin–Hochberg method) was set to 0.01. Gene Ontology (GO) terms were used for functional annotation. A p-value < 0.05 was compiled with Nexus Expression and associated with different cellular functions using an in-house model as previously described⁴⁵. Human Protein Atlas (<https://www.proteinatlas.org>) was used to identify thyroid-specific genes.

Tandem mass spectrometry (LC–MS/MS) analysis. Total cellular proteins were extracted from thyroid and plasma samples and labelled with isobaric labels, TMT 10-plex (Thermo Fisher Scientific, Waltham, MA, USA). Thyroid samples for each irradiated group and controls were pooled, respectively. The plasma samples were pooled in the same manner. Tandem mass spectrometry (LC–MS/MS) was performed at the Proteomics Core Facility at University of Gothenburg (Gothenburg, Sweden) as previously described²⁴. Differentially expressed proteins were identified at ≥ 1.5 -fold change. The (DAVID) bioinformatics resource tool (<https://david.ncifcrf.gov/>) was used for functional protein annotation. Proteins were associated with GO terms and categorised in a similar manner as the RNA microarray data. Human Protein Atlas (<https://www.proteinatlas.org>) was used to identify thyroid-specific proteins.

Ingenuity pathway analysis (IPA). Ingenuity pathway analysis (IPA) software (Ingenuity Systems, Redwood City, USA) was used to analyse affected canonical pathways, biological functions and upstream regulators for the identified transcripts and proteins. Fisher's exact test ($p < 0.05$) was used for statistical significance analyses. Upstream regulators with z-score > 2 or z-score < -2 were denoted as activated or inhibited, respectively.

Hormonal assays. Thyroid hormone levels were measured in plasma from young and adult rats, 9 months after exposure, and from corresponding controls. The plasma concentration of thyroid stimulating hormone (TSH) and triiodothyronine (T3) were measured using ELISA kits (CSB-E05085r, CSB-E05115r, Cusabio, Hou-

ston, TX, USA). Thyroxine (T4) levels were measured using ELISA kit (GWB-39U2L8, GenWay, San Diego, CA, USA). All ELISA plates were read on Victor 31420 multilabel plate counter (Perkin Elmer, Waltham, MA, USA).

Histological analysis of thyroid tissue. In a group of other rats, treated in a similar way, thyroid tissue was surgically removed from each rat after twelve months. Thyroid tissue was fixed in formalin and imbedded in paraffin for histological analysis. A certified pathologist evaluated thyroid tissue morphology, abnormal tissue structure, and the presence of tumour cells, using paraffin sections (4 µm) stained with haematoxylin and eosin.

Data availability

The mRNA datasets created and analysed are available at NCBI's Gene Expression Omnibus⁶¹ and are accessible through GEO Series accession number GSE146051 <https://www.ncbi.nlm.nih.gov/geo/query/acc.cgi?acc=GSE146051>. The mass spectrometry proteomics data have been deposited to the ProteomeXchange Consortium via the PRIDE⁶² partner repository with the dataset identifier PXD017715. The data for the Y9 group has been published elsewhere²⁴.

Received: 4 March 2021; Accepted: 18 January 2022

Published online: 08 February 2022

References

- IAEA. Chernobyl's legacy: Health, environmental and socio-economic impacts and recommendations to the governments of belarus, the russian federation and ukraine the chernobyl forum International Atomic Energy Agency (IAEA)2005 [INIS-XA-798]. 52]. http://www.iaea.org/NewsCenter/Focus/Chernobyl/pdfs/05-28601_Chernobyl.pdf. http://inis.iaea.org/search/search.aspx?orig_q=RN:36093263. Accessed 30 Nov 2020.
- UNSCEAR. Evaluation of data on thyroid cancer in regions affected by the chernobyl accident. *UNSCEAR Rep.* 11–21 (2018).
- Sinclair, W. K. & Morton, R. A. X-ray and ultraviolet sensitivity of synchronized chinese hamster cells at various stages of the cell cycle. *Biophys. J.* 5, 1–25 (1965).
- Hall, E. J., Brown, J. M. & Cavanagh, J. Radiosensitivity and the oxygen effect measured at different phases of the mitotic cycle using synchronously dividing cells of the root meristem of vicia faba. *Radiat. Res.* 35(3), 622–634 (1968).
- Cardis, E. & Hatch, M. The chernobyl accident—An epidemiological perspective. *Clin. Oncol. (R. Coll. Radiol.)* 23(4), 251–260 (2011).
- Hatch, M. & Cardis, E. Somatic health effects of chernobyl: 30 years on. *Eur. J. Epidemiol.* 32(12), 1047–1054 (2017).
- Ng, J. & Shuryak, I. Minimizing second cancer risk following radiotherapy: Current perspectives. *Cancer Manag. Res.* 7, 1–11 (2015).
- Hall, P., Mattsson, A. & Boice, J. D. Jr. Thyroid cancer after diagnostic administration of iodine-131. *Radiat. Res.* 145(1), 86–92 (1996).
- Dinets, A. *et al.* Clinical, genetic, and immunohistochemical characterization of 70 ukrainian adult cases with post-chornobyl papillary thyroid carcinoma. *Eur. J. Endocrinol.* 166(6), 1049–1060 (2012).
- Suzuki, K., Mitsutake, N., Saenko, V. & Yamashita, S. Radiation signatures in childhood thyroid cancers after the chernobyl accident: Possible roles of radiation in carcinogenesis. *Cancer Sci.* 106(2), 127–133 (2015).
- Philchenkov, A. A. & Balcer-Kubiczek, E. K. Molecular markers of apoptosis in cancer patients exposed to ionizing radiation: The post-chornobyl view. *Exp. Oncol.* 38(4), 224–237 (2016).
- Kaiser, J. C. *et al.* Integration of a radiation biomarker into modeling of thyroid carcinogenesis and post-chernobyl risk assessment. *Carcinogenesis* 37(12), 1152–1160 (2016).
- Nikiforov, Y. E., Koshoffer, A., Nikiforova, M., Stringer, J. & Fagin, J. A. Chromosomal breakpoint positions suggest a direct role for radiation in inducing illegitimate recombination between the *el1* and *ret* genes in radiation-induced thyroid carcinomas. *Oncogene* 18(46), 6330–6334 (1999).
- Abend, M. *et al.* Iodine-131 dose-dependent gene expression: Alterations in both normal and tumour thyroid tissues of post-chernobyl thyroid cancers. *Br. J. Cancer.* 109(8), 2286–2294 (2013).
- Akulevich, N. M. *et al.* Polymorphisms of DNA damage response genes in radiation-related and sporadic papillary thyroid carcinoma. *Endocr. Relat. Cancer.* 16(2), 491–503 (2009).
- Selmansberger, M. *et al.* Clip2 as radiation biomarker in papillary thyroid carcinoma. *Oncogene* 34(30), 3917–3925 (2015).
- Lando, A. *et al.* Serum thyroglobulin as a marker of thyroid neoplasms after childhood cancer. *Acta Paediatr.* 92(11), 1284–1290 (2003).
- Schneider, A. B. *et al.* Continuing occurrence of thyroid nodules after head and neck irradiation. Relation to plasma thyroglobulin concentration. *Ann. Intern. Med.* 94(2), 176–180 (1981).
- Indrasena, B. S. Use of thyroglobulin as a tumour marker. *World J. Biol. Chem.* 8(1), 81–85 (2017).
- Langen, B., Rudqvist, N., Spetz, J., Helou, K. & Forssell-Aronsson, E. Deconvolution of expression microarray data reveals ¹³¹I-induced responses otherwise undetected in thyroid tissue. *PLoS ONE* 13(7), e0197911 (2018).
- Langen, B., Rudqvist, N., Parris, T. Z., Helou, K. & Forssell-Aronsson, E. Circadian rhythm influences genome-wide transcriptional responses to (131)I in a tissue-specific manner in mice. *EJNMMI Res.* 5(1), 75 (2015).
- Rudqvist, N. *et al.* Transcriptional response to ¹³¹I exposure of rat thyroid gland. *PLoS ONE* 12(2), e0171797 (2017).
- Rudqvist, N. *et al.* Dose-specific transcriptional responses in thyroid tissue in mice after (131)I administration. *Nucl. Med. Biol.* 42(3), 263–268 (2015).
- Larsson, M. *et al.* Long-term transcriptomic and proteomic effects in Sprague Dawley rat thyroid and plasma after internal low dose ¹³¹I exposure. *PLoS ONE* 15(12), e0244098 (2020).
- Amundson, S. A. & Fornace, A. J. Jr. Gene expression profiles for monitoring radiation exposure. *Radiat. Prot. Dosimetry.* 97(1), 11–16 (2001).
- Stelzer, G. *et al.* The genecards suite: From gene data mining to disease genome sequence analyses. *Curr. Protoc. Bioinform.* 54, 1–30 (2016).
- Yoshida, K. *et al.* Clinical utility of red blood cell carbonic anhydrase I and zinc concentrations in patients with thyroid diseases. *Metabolism* 40(10), 1048–1051 (1991).
- Rudqvist, N. *et al.* Gene expression signature in mouse thyroid tissue after (131)I and (211)at exposure. *EJNMMI Res.* 5(1), 59 (2015).
- Moll, R., Divo, M. & Langbein, L. The human keratins: Biology and pathology. *Histochem. Cell Biol.* 129(6), 705–733 (2008).
- Lamberti, A. *et al.* Analysis of interaction partners for eukaryotic translation elongation factor 1a m-domain by functional proteomics. *Biochimie* 93(10), 1738–1746 (2011).

31. Byun, H. O. *et al.* Cathepsin d and eukaryotic translation elongation factor 1 as promising markers of cellular senescence. *Cancer Res.* **69**(11), 4638–4647 (2009).
32. Daoud, S. A., Esmail, R. S., Hareedy, A. A. & Khalil, A. Stromal modulation and its role in the diagnosis of papillary patterned thyroid lesions. *Asian Pac. J. Cancer Prev.* **16**(8), 3307–3312 (2015).
33. Vriens, M. R. *et al.* Clinical and molecular features of papillary thyroid cancer in adolescents and young adults. *Cancer* **117**(2), 259–267 (2011).
34. Hou, J., Shan, H., Zhang, Y., Fan, Y. & Wu, B. M(6)a rna methylation regulators have prognostic value in papillary thyroid carcinoma. *Am. J. Otolaryngol.* **41**(4), 102547 (2020).
35. Galli, M. *et al.* Proteomic profiles of thyroid tumors by mass spectrometry-imaging on tissue microarrays. *Biochim. Biophys. Acta Proteins Proteom.* **1865**(7), 817–827 (2017).
36. Najafian, A. *et al.* Ras mutations, and ret/ptc and pax8/ppar-gamma chromosomal rearrangements are also prevalent in benign thyroid lesions: Implications thereof and a systematic review. *Thyroid* **27**(1), 39–48 (2017).
37. Bhajjee, F. & Nikiforov, Y. E. Molecular analysis of thyroid tumors. *Endocr. Pathol.* **22**(3), 126–133 (2011).
38. Mullur, R., Liu, Y. Y. & Brent, G. A. Thyroid hormone regulation of metabolism. *Physiol. Rev.* **94**(2), 355–382 (2014).
39. Srikantia, N. *et al.* How common is hypothyroidism after external radiotherapy to neck in head and neck cancer patients?. *Indian J. Med. Paediatr. Oncol.* **32**(3), 143–148 (2011).
40. Lisabeth, E. M., Falivelli, G., Pasquale, E. B. Eph receptor signaling and ephrins. *Cold Spring Harb. Perspect. Biol.* **5**(9), 1–20 (2013).
41. Turner, C. E. Paxillin and focal adhesion signalling. *Nat. Cell Biol.* **2**(12), E231–E236 (2000).
42. Giancotti, F. G. & Ruoslahti, E. Integrin signaling. *Science* **285**(5430), 1028–1032 (1999).
43. Yu, J., Mai, W., Cui, Y. & Kong, L. Key genes and pathways predicted in papillary thyroid carcinoma based on bioinformatics analysis. *J. Endocrinol. Invest.* **39**(11), 1285–1293 (2016).
44. Pordanjani, S. M. & Hosseinimehr, S. J. The role of nf-kb inhibitors in cell response to radiation. *Curr. Med. Chem.* **23**(34), 3951–3963 (2016).
45. Langen, B. *et al.* Comparative analysis of transcriptional gene regulation indicates similar physiologic response in mouse tissues at low absorbed doses from intravenously administered 211at. *J. Nucl. Med.* **54**(6), 990–998 (2013).
46. Rudqvist N. Radiobiological effects of the thyroid gland. University of Gothenburg. https://gupea.ub.gu.se/bitstream/2077/38006/1/gupea_2077_38006_1.pdf. Accessed 30 Nov 2020. (2015).
47. Marchetti, F., Coleman, M. A., Jones, I. M. & Wytrobek, A. J. Candidate protein biosimeters of human exposure to ionizing radiation. *Int. J. Radiat. Biol.* **82**(9), 605–639 (2006).
48. Cahoon, E. K. *et al.* Factors associated with serum thyroglobulin levels in a population living in belarus. *Clin. Endocrinol. (Oxf.)* **79**(1), 120–127 (2013).
49. Robbins, J. & Schneider, A. B. Radioiodine-induced thyroid cancer: Studies in the aftermath of the accident at chernobyl. *Trends Endocrinol. Metab.* **9**(3), 87–94 (1998).
50. Cahoon, E. K. *et al.* Risk of thyroid nodules in residents of belarus exposed to chernobyl fallout as children and adolescents. *J. Clin. Endocrinol. Metab.* **102**(7), 2207–2217 (2017).
51. Tronko, M. *et al.* Thyroid cancer in ukraine after the chernobyl accident (in the framework of the ukraine-us thyroid project). *J. Radiol. Prot.* **32**(1), N65–N69 (2012).
52. Yamashita, S., Suzuki, S., Suzuki, S., Shimura, H. & Saenko, V. Lessons from fukushima: Latest findings of thyroid cancer after the fukushima nuclear power plant accident. *Thyroid* **28**(1), 11–22 (2018).
53. Peters, K. O. *et al.* Factors associated with serum thyroglobulin in a ukrainian cohort exposed to iodine-131 from the accident at the chernobyl nuclear plant. *Environ. Res.* **156**, 801–809 (2017).
54. Selmansberger, M. *et al.* Dose-dependent expression of clip2 in post-chernobyl papillary thyroid carcinomas. *Carcinogenesis* **36**(7), 748–756 (2015).
55. Dom, G. *et al.* A gene expression signature distinguishes normal tissues of sporadic and radiation-induced papillary thyroid carcinomas. *Br. J. Cancer.* **107**(6), 994–1000 (2012).
56. Takahashi, M. *et al.* The foxe1 locus is a major genetic determinant for radiation-related thyroid carcinoma in chernobyl. *Hum. Mol. Genet.* **19**(12), 2516–2523 (2010).
57. Asa, S. L. How familial cancer genes and environmentally induced oncogenes have changed the endocrine landscape. *Mod. Pathol.* **14**(3), 246–253 (2001).
58. Stein, L. *et al.* Copy number and gene expression alterations in radiation-induced papillary thyroid carcinoma from chernobyl pediatric patients. *Thyroid* **20**(5), 475–487 (2010).
59. Spetz, J., Rudqvist, N. & Forssell-Aronsson, E. Biodistribution and dosimetry of free 211at, 125i- and 131i- in rats. *Cancer Biother. Radiopharm.* **28**(9), 657–664 (2013).
60. Rao-Rupanagudi, S., Heywood, R. & Gopinath, C. Age-related changes in thyroid structure and function in Sprague-Dawley rats. *Vet. Pathol.* **29**(4), 278–287 (1992).
61. Edgar, R., Domrachev, M. & Lash, A. E. Gene expression omnibus: Ncbi gene expression and hybridization array data repository. *Nucleic Acids Res.* **30**(1), 207–210 (2002).
62. Perez-Riverol, Y. *et al.* The pride database and related tools and resources in 2019: Improving support for quantification data. *Nucleic Acids Res.* **47**(D1), D442–D450 (2019).

Acknowledgements

The authors would like to thank Lab techs Lilian Karlsson and Ann Wikström for their skilled technical assistance, and Daniella Pettersson for ELISA analyses. We thank the Core facility at Novum, BEA, Bioinformatics and Expression Analysis, which is supported by the board of research at the Karolinska Institute and the research committee at the Karolinska University Hospital. Quantitative proteomic analysis was performed at the Proteomics Core Facility at Sahlgrenska Academy, University of Gothenburg. The Proteomics Core Facility is grateful to the Inga-Britt and Arne Lundberg Research Foundation for the donation of the Orbitrap Fusion Tribrid MS instrument.

Author contributions

M.L., N.R., J.S., B.L. and E.F.A. contributed to the conceptualization. M.L. and N.R. performed the data curation. M.L., J.S., T.Z.P. and B.L. made the formal analysis. M.L., N.R. and E.F.A. were responsible for the founding acquisition. M.L., N.R., J.S., T.Z.P. and B.L. performed the investigation. M.L., N.R., J.S., T.Z.P., B.L., K.H. and E.F.A. choose the methodology. K.H. and E.F.A. administered and supervised the project. M.L., K.H. and E.F.A. validated the project. M.L. wrote the original draft. M.L., N.R., J.S., T.Z.P., B.L., K.H. and E.F.A. reviewed and edited the original draft.

Funding

Open access funding provided by University of Gothenburg. This study was supported by Grants from Bio-CARE—a National Strategic Research Program at the University of Gothenburg, the Swedish Cancer Society (Grant no. 3427), the Swedish Research Council (Grant no. 21073), the Swedish state under the agreement between the Swedish government and the county councils—the ALF-agreement (ALFGBG-725031), Swedish Radiation Safety Authority (SSM), the King Gustav V Jubilee Clinic Cancer Research Foundation, the Sahlgrenska University Hospital Research Funds, the Assar Gabrielsson Cancer Research Foundation, the Adlerbertska Research Foundation, the Knut and Alice Wallenberg Foundation, the Royal Society of Arts and Sciences in Gothenburg (KVVVS), and the Wilhelm and Martina Lundgren Research Foundation.

Competing interests

The authors declare no competing interests.

Additional information

Supplementary Information The online version contains supplementary material available at <https://doi.org/10.1038/s41598-022-06071-4>.

Correspondence and requests for materials should be addressed to M.L.

Reprints and permissions information is available at www.nature.com/reprints.

Publisher's note Springer Nature remains neutral with regard to jurisdictional claims in published maps and institutional affiliations.



Open Access This article is licensed under a Creative Commons Attribution 4.0 International License, which permits use, sharing, adaptation, distribution and reproduction in any medium or format, as long as you give appropriate credit to the original author(s) and the source, provide a link to the Creative Commons licence, and indicate if changes were made. The images or other third party material in this article are included in the article's Creative Commons licence, unless indicated otherwise in a credit line to the material. If material is not included in the article's Creative Commons licence and your intended use is not permitted by statutory regulation or exceeds the permitted use, you will need to obtain permission directly from the copyright holder. To view a copy of this licence, visit <http://creativecommons.org/licenses/by/4.0/>.

© The Author(s) 2022